An Improved Time Synchronization Scheme Using Timestamp-Free Mechanism for 5G-Advanced Networks

Heng Wang*, Wenjun Zhang*, Yuxi Deng*, and Xiaojiang Liu[†]
*Key Laboratory of Industrial Internet of Things and Networked Control,
Chongqing University of Posts and Telecommunications, Chongqing 400065, China

†Chongqing Key Laboratory of Optoelectronic Information Sensing and Transmission Technology,
Chongqing University of Posts and Telecommunications, Chongqing 400065, China
Email: wangheng@cqupt.edu.cn, zhangwenjun202505@163.com, dyx190016@163.com, liuxiaojiang1024@163.com

Abstract—As a critical transitional phase in the evolution from 5G to 6G, 5G-Advanced (5G-A) aims to enhance existing 5G network performance and support the digital transformation of industrial applications. It has seen widespread adoption in sectors such as smart manufacturing, autonomous driving, and telemedicine. In 5G-A networks, precise time synchronization is crucial for maintaining the accuracy of wireless communication and ensuring network stability. Synchronization precision directly affects service reliability and safety in real-time applications. However, the existing synchronization mechanisms in 5G-A networks are primarily based on signaling interactions, which are inherently limited by the characteristics of signaling itself and thus face challenges in fulfilling the requirements of highprecision time synchronization. To address these limitations, an improved time synchronization method is proposed in this paper for 5G-A networks. The process is implemented based on the OpenAirInterface (OAI) 5G protocol stack and introduces a synchronization mechanism that integrates both user-plane data and control-plane signaling. Experimental results demonstrate that the proposed method significantly improves synchronization accuracy when compared with existing mechanisms and is capable of effectively meeting the demands of high-precision time synchronization in next-generation network scenarios.

Index Terms—5G-Advanced, time synchronization, timestampfree synchronization, HARQ mechanism.

I. INTRODUCTION

As an evolution of 5G networks, 5G-Advanced (5G-A) will further promote the development of mobile communication technology and provide higher transmission rates, lower network latency, wider user coverage, and more flexible network architecture [1]. Owing to its marked enhancements in bandwidth, latency, and reliability, 5G-A has been extensively deployed in industrial systems for applications such as production monitoring, remote operation and maintenance, intelligent manufacturing, and edge-computing collaboration. Such deployments are known to afford robust support for the real-time interconnection and large-scale data-processing requirements of industrial equipment. As a key technology for the stable operation of 5G-A networks, time synchronization

This work was supported by the National Natural Science Foundation of China (Grant No. U23B2003), and by the Natural Science Foundation of Chongqing, China (Grant No. CSTB2024NSCQ-LZX0127).

technology ensures that the network responds to application requirements in real-time through precise timing control and ensures that data packets arrive on time along the predetermined path. In high-precision scenarios such as autonomous driving, telemedicine, industrial Internet of Things, and virtual reality, high requirements are placed on the accuracy of time synchronization.

Time synchronization has become a critical research focus in the evolution of 5G-A networks, driven by the stringent requirements of emerging applications such as ultra-reliable low-latency communications (URLLC) and time-sensitive networking (TSN). Traditional synchronization methods such as Global Navigation Satellite Systems (GNSS), atomic clocks, the Precision Time Protocol (PTP), and the Network Time Protocol (NTP) have been widely deployed across various network infrastructures. However, these conventional approaches face significant challenges in adapting to the dynamic and heterogeneous environments of 5G and 5G-A networks. In particular, challenges such as GNSS signal blockage, the limited precision of NTP, and the high deployment cost of atomic clocks constrain their effectiveness in wireless scenarios [2]-[4]. Therefore, there is a urgent need to develop advanced synchronization techniques capable of meeting the high-precision, low-latency requirements of next-generation wireless systems.

In response to these challenges, researchers have proposed various innovative approaches tailored to the unique requirements of 5G and 5G-A networks in order to achieve high-precision synchronization. The synchronization mechanisms within New Radio (NR) networks, including clock, phase, and frequency synchronization, are systematically elucidated in [5], laying a theoretical foundation for 5G time synchronization technologies. The authors in [6] present a comprehensive overview of three primary synchronization paradigms for 5G-A networks: direct air interface synchronization, integration with the TSN protocol, and PTP-based network synchronization.

The authors in [7] conducted an in-depth analysis of the synchronization architecture introduced in 3GPP Release 17,

focusing on timing errors occurring in both the transmission and wireless segments of the network. In [8], the authors explore the potential of leveraging timing advance (TA) for critical machine-type communications (cMTC) in 5G networks, assessing the impact of multipath propagation on TA accuracy and proposing a conceptual framework for synchronization using TA and broadcast signaling.

A 5G adaptation scheme based on the Reference Broadcast Infrastructure Synchronization (RBIS) protocol is proposed in [9], enabling wide-area node synchronization by leveraging the broadcast capabilities of the 5G NR control plane. To meet sub-microsecond accuracy requirements, an enhanced TAPv2-based method is proposed in [10], incorporating a specially designed SIB9-r16t signaling structure, significantly improving synchronization precision and stability. An alternative approach is presented in [11], which proposes an absolute synchronization scheme based on timing messages. By embedding the synchronization process into the random access procedure and designing the frame structure of the timing messages, the clock frequency and phase offset are jointly estimated, achieving high accuracy with low computational complexity in simulations.

Although substantial progress has been made in time synchronization for 5G and 5G-A networks, most existing methods still rely primarily on signaling-based mechanisms, such as two-way interactive synchronization via random access procedures or one-way synchronization through System Information Block (SIB) broadcasts. However, these signaling-based approaches are inherently limited and fall short of meeting the stringent requirements for high-precision synchronization in specific applications.

To address this issue, this paper proposes a novel synchronization method that enhances existing mechanisms by estimating clock frequency offset and fixed delay through the integration of user data streams with the Hybrid Automatic Repeat Request (HARQ) mechanism. Additionally, it calculates the phase offset in conjunction with control signaling, thereby improving synchronization accuracy. The main contributions of this work are as follows:

- The clock frequency offset estimation is integrated into the data interaction of the 5G-A network, enabling clock frequency offset estimation without the need for signaling frames or dedicated synchronization frames, thereby reducing synchronization overhead.
- The traditional System Information Block 9 (SIB9) signaling is functionally extended to design the enhanced SIB9-sync signaling, enabling the User Equipment (UE) to acquire clock synchronization parameters broadcast by the Next Generation Node B (gNB). Upon reception, the UE utilizes these parameters to calculate the clock phase offset.

The rest of this paper consists of the following sections. Section II presents the synchronization process and system model. Section III describes the improved time synchronization solution for the 5G-A network. Section IV implements the

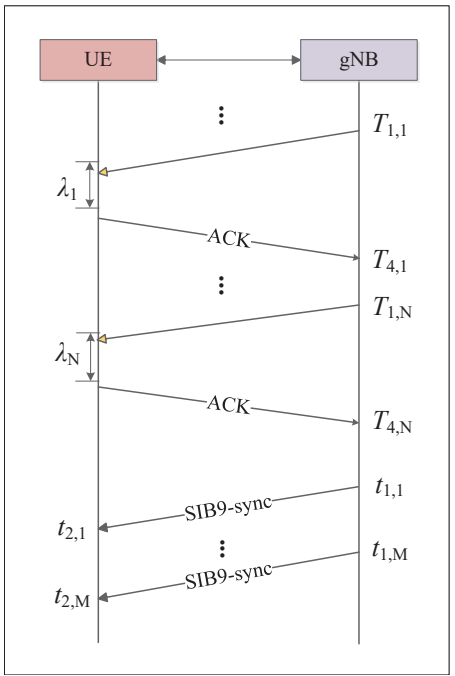


Fig. 1. Overall flow chart of the improved time synchronization method.

proposed scheme and provides experimental results. Finally, Section V concludes the paper.

II. SYNCHRONIZATION PROCESS AND SYSTEM MODEL

This section provides a detailed analysis of the synchronization procedure of the proposed method, followed by a description of the corresponding system framework.

A. Synchronization Process

Before initiating synchronization, an initialization procedure must be completed to ensure that the UE successfully accesses the gNB and that the relevant clock synchronization parameters are properly configured. Once initialization is complete, the system proceeds to the formal synchronization phase, with the corresponding control flow illustrated in Fig. 1.

First, when the synchronization period is reached, the gNB activates the HARQ mechanism and executes a timestamp-free synchronization algorithm based on real-time data traffic to estimate the clock frequency offset and fixed delay. Second, upon completing the synchronization computation, the gNB transmits the estimated synchronization parameters to the UE through the enhanced SIB9-sync signaling, ensuring accurate and timely dissemination of synchronization information. Finally, after receiving and parsing the synchronization parameters, the UE performs one-way clock synchronization using the SIB9-sync broadcast and subsequently calculates the clock phase offset.

B. System Model

To implement the proposed improved time synchronization method, a comprehensive software architecture is designed, as illustrated in Fig. 2. In this architecture, the gNB operates as the master clock node and synchronizes with a high-precision time source via the PTP protocol, while the UE acts as

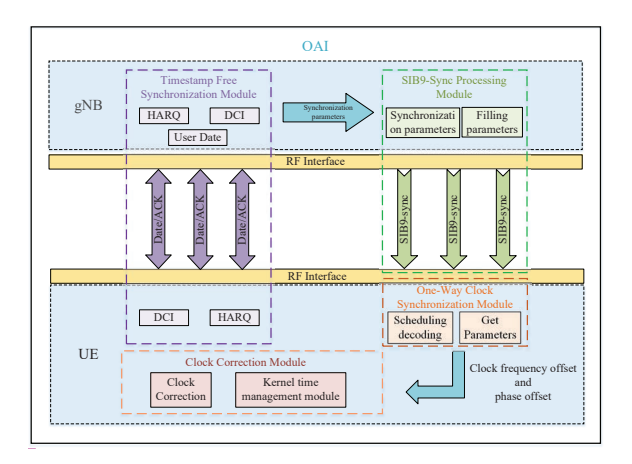


Fig. 2. improved time synchronization method adaptation architecture.

the slave clock node, achieving network-wide time alignment through an air-interface-based synchronization mechanism.

The software framework is developed on the OpenAirInterface (OAI) 5G experimental platform and comprises four core modules: the timestamp-free synchronization module, the SIB9-sync processing module, the one-way clock synchronization module, and the clock correction module. The functionalities of each module are detailed as follows:

- Timestamp-Free Synchronization Module: This module is integrated into the HARQ protocol. On the gNB side, ACK/NACK feedback timestamps are obtained by monitoring the HARQ process at the MAC layer, and the clock frequency offset and fixed delay are calculated based on the timestamps of the corresponding transmitted data captured at the MAC layer.
- SIB9-sync Processing Module: This module generates enhanced signaling carrying the estimated clock frequency offset and fixed delay using ASN.1 encoding. It is also responsible for transmitting the signaling on the gNB side.
- One-Way Clock Synchronization Module: On the UE side, this module parses the reference timestamp and the local reception timestamp from the received SIB9-sync signaling. A least-squares estimation model is then applied, combined with the fixed delay, to compute the clock phase offset.
- Clock Correction Module: This module performs time offset correction by invoking the Linux kernel time subsystem API and mitigates frequency drift by dynamically adjusting the oscillator compensation step.

III. ADAPTATION SCHEME

This section proposes an improved time synchronization scheme specifically designed to meet the high-precision requirements of 5G-A networks.

A. Adaptation of Timestamp-Free Synchronization Method

During 5G downlink data transmission, the HARQ process control unit is triggered by the gNB each time a trans-

port block is sent to the UE. Upon decoding the Downlink Control Information (DCI) Format 1_1 on the Physical Downlink Control Channel (PDCCH), the UE selects a specific time slot from the k1 offset value set, predefined by the Radio Resource Control (RRC) layer, based on the pdsch_to_harq_feedback_timing_indicator. The corresponding HARQ-ACK/NACK information is then fed back to the gNB within the designated absolute time slot window.

The dynamic timing configuration of the HARQ mechanism is inherently coupled with the timestamp-free synchronization method based on dynamic response. When the feedback time slot parameters are dynamically configured through DCI Format 1_1, a dynamic response time model is implicitly constructed between the enslaver and slave clocks, thereby enhancing the compatibility with the proposed synchronization approach.

As a result, the timestamp-free synchronization method based on dynamic response is seamlessly embedded into the 5G downlink transmission process. By leveraging the HARQ protocol and DCI signaling, a signaling-free synchronization scheme applicable to 5G-A networks is effectively realized.

The main process is as follows: first, upon receiving the UE data request, the waiting time for the UE to return the confirmation frame is configured by the gNB via DCI signaling, and a response data packet is transmitted by the gNB at its local time. The data packet contains only the necessary communication data and does not include any timestamp information. Secondly, after the data packet transmitted by the gNB is received by the UE, a fixed time interval, as specified by the feedback time parameters in the DCI signaling, is observed before a response message is generated and transmitted by the UE based on the decoding process. Finally, upon successful receipt of the feedback response message from the UE, the gNB records the arrival time of the response message.

The dynamic timestamp-free synchronization method uses a linear clock model to calculate the time interval required for a round-trip transmission. The mathematical model is defined as

$$T_{4,i} - T_{1,i} = \frac{\lambda_i}{1 + \varepsilon^{(GU)}} + 2\mu + \xi_i^{(GU)} + \xi_i^{(UG)},$$
 (1)

where $T_{4,i}$ represents the time at which the gNB receives the ACK, $T_{1,i}$ denotes the time at which the gNB sends data to the UE, λ_i is the waiting time interval in the current cycle, $\varepsilon^{(GU)}$ stands for the initial clock frequency offset between the gNB and the UE, μ represents the fixed delay introduced during the wireless communication process, and $\xi_i^{(GU)}$ and $\xi_i^{(UG)}$ denote the random delays introduced in the gNB to UE and UE to gNB links, respectively.

Assuming that the timestamp-free interaction based on dynamic response is executed N times, the time data $\{T_{1,i},T_{4,i}\}_{i=1}^N$ recorded at the gNB side are utilized, where N denotes the number of executions of the two-way information interaction. The corresponding mathematical model is subsequently solved using the maximum likelihood estimation

TABLE I SIB9-SYNC FUNCTION TABLE

Field	Function Description
TimeInfo	UTC time of SIB9 transmission
dayLightSavingTime	Indicates whether and how daylight saving time is applied
leapSeconds	Leap second offset between GPS and UTC
SynchronousState	Indicates whether the system is currently synchronized
UE_id	The UE currently being synchronized with
Offset	Clock frequency offset
Delay	Fixed delay
localTimeOffset	Offset between UTC and local time
lateNonCriticalExtension	Reserved field for signaling compatibility
ReferenceTimeInfo-r16	Provides time with 10-nanosecond granularity

method. The $\varepsilon^{(GU)}$ can be modeled as

$$\hat{\varepsilon} = \frac{N \sum_{i=1}^{N} \lambda_i^2 - (\sum_{i=1}^{N} \lambda_i)^2}{N \sum_{i=1}^{N} (T_{4,i} - T_{1,i}) \lambda_i - \sum_{i=1}^{N} \lambda_i \sum_{i=1}^{N} (T_{4,i} - T_{1,i})}, \quad (2)$$

and the $\hat{\mu}$ is calculated by

$$\hat{u} = \frac{\sum_{i=1}^{N} \lambda_i^2 \sum_{i=1}^{N} (T_{4,i} - T_{1,i}) - \sum_{i=1}^{N} \lambda_i \sum_{i=1}^{N} (T_{4,i} - T_{1,i}) \lambda_i}{2N \sum_{i=1}^{N} \lambda_i^2 - 2\left(\sum_{i=1}^{N} \lambda_i\right)^2}.$$
 (3)

B. Design of SIB9-sync Signaling

In order to enable the UE to perform time correction accurately, the synchronization parameters calculated at the gNB side must be delivered to the UE. In the 5G NR system, the gNB periodically broadcasts system information messages, among which the SIB9 is primarily used to provide either the GPS reference time or the gNB local time to assist in time synchronization. Building upon this functionality, an enhanced SIB9-sync signaling scheme is proposed. This scheme extends the reserved fields of SIB9 by adding the following fields: SynchronousState, UE_id, Offset, and Delay. The field descriptions of the SIB9-sync signaling are summarized in Table I.

The SynchronousState field indicates whether the system is currently in a synchronized state. A value of true instructs the UE to process the subsequent synchronization parameters, whereas a value of false signals that the synchronization information is invalid and may be safely ignored, thereby reducing unnecessary processing overhead.

Since a gNB may simultaneously serve multiple UEs, the UE_id field is used to identify the intended recipient. This field carries the identifier previously assigned to the UE during registration with the gNB, ensuring that each UE accurately receives and utilizes its corresponding synchronization parameters.

The Offset field carries the clock frequency offset estimated by the gNB. The UE uses this information to align its clock frequency with that of the gNB. Besides, the Delay field conveys the fixed delay estimated at the gNB side. Combined with the received SIB9-sync signaling, this enables the UE to perform one-way time synchronization and calculate the clock phase offset for precise clock correction.

C. Adaptation of One-Way Clock Synchronization Method

In order to achieve accurate calibration of the UE clock. one-way clock synchronization must be performed based on the SIB9-sync signaling periodically broadcast by the gNB. During the phase offset calculation process, the fixed delay parameter embedded within the SIB9-sync signaling is required as an essential input. Accordingly, the SIB9-sync signaling is integrated with the one-way clock synchronization mechanism, enabling precise estimation of the clock phase offset on the UE side. First, the SIB9-sync signaling is periodically transmitted by the gNB according to the time-frequency resources specified in SIB1. Then, the arrival time of the signaling at the UE is locally recorded, along with the transmission timestamp embedded within the received SIB9-sync signaling. Finally, when the SynchronousState field is set to true and both the Delay and Offset fields are non-zero, one-way time synchronization is performed. The previously recorded time information and the Delay parameter are utilized to compute the clock phase offset, enabling accurate synchronization of the UE clock with that of the gNB.

Based on the time data collected at the UE side, the transmission time of the gNB can be modeled mathematically. The corresponding expression result is

$$t_{1,i} = (1 + \varepsilon^{(\text{UG})})(t_{1,i} - \mu - \xi_i^{(GU)}) + \gamma^{(\text{UG})}, \tag{4}$$

where $\gamma^{(\mathrm{UG})}$ is the clock phase offset between UE and gNB, $t_{1,i}$ denotes the time at which the signaling is transmitted by the gNB. After M rounds of communication, a series of timestamp pairs are recorded on the UE side. The clock frequency offset and fixed delay are obtained from the SIB9-sync signaling. Based on this information, the clock phase offset can be estimated using the least squares method. The relevant calculation formula is defined as

$$\gamma^{(\text{UG})} = \frac{\sum_{i=1}^{M} t_{1,i} \sum_{i=1}^{M} (t_{1,i}t_{2,i}) - \sum_{i=1}^{M} (t_{1,i})^{2} \sum_{i=1}^{M} t_{2,i}}{M \sum_{i=1}^{M} (t_{1,i}t_{2,i}) - \sum_{i=1}^{M} t_{1,i} \sum_{i=1}^{M} t_{2,i}} + \frac{\mu \left[M \sum_{i=1}^{M} (t_{1,i})^{2} - \left(\sum_{i=1}^{M} t_{1,i} \right)^{2} \right]}{M \sum_{i=1}^{M} (t_{1,i}t_{2,i}) - \sum_{i=1}^{M} t_{1,i} \sum_{i=1}^{M} t_{2,i}}, \tag{5}$$

where $t_{2,i}$ denotes the time at which it is received by the UE.

IV. IMPLEMENTATION AND TESTING

In this section, an experimental platform is constructed to evaluate the proposed improved time synchronization solution. Both functional and performance aspects of the method are verified and tested. Functional verification is conducted through log analysis, network packet capture, and related diagnostic tools. Performance evaluation focuses primarily on synchronization accuracy and resource consumption.



Fig. 3. Physical picture of improved time synchronization method system test

A. Implementation

As an enhanced and evolved version of 5G technology, the core architecture of the 5G-A network still follows the framework defined in the 3GPP Release 15/16 specifications, mainly focusing on protocol stack optimizations to improve key performance indicators. Therefore, in subsequent experiments, the 5G experimental platform is adopted as a representative environment to implement and validate the improved time synchronization method for the 5G-A network.

In this study, the proposed time synchronization scheme is implemented on the OAI platform to evaluate its feasibility. The experimental setup is illustrated in Fig. 3. Two embedded microcomputers and a personal computer are employed to construct the OAI gNB, OAI UE, and OAI 5GC, respectively. Additionally, two USRP B210 software-defined radios are used to provide wireless transceiver functionality. The OAI 5GC was deployed on an Ubuntu 18.04 (Bionic) Linux system. utilizing Python 3.6.9 as the runtime environment. A MySQL 5.0 database was employed for data management, and Docker containers were used to facilitate rapid deployment. The system was operated on an Intel Core i5-8500 CPU running at 3.00 GHz with 6 physical cores. The OAI gNB and OAI UE were both deployed on Ubuntu 24.04 Linux systems, each using Python 3.6.9 as the development environment. A lowlatency kernel, specifically Linux 5.4.0-120-low-latency, was adopted to reduce system delay. To ensure stable performance under high load, the CPU turbo boost feature was disabled, allowing the system to operate at a fixed frequency. The hardware platform was based on an Intel Core i9-11900 CPU running at 2.50 GHz, featuring 8 physical cores and 16 threads.

B. Experimental Results

The functions, including the timestamp-free mechanism, the SIB9-sync signaling frame, and one-way time synchronization, have been validated through the proposed improved time synchronization adaptation scheme. The architecture of the timestamp-free mechanism is illustrated in Fig. 4(a). As illustrated, the system can accurately capture both transmission and reception timestamps, enabling simultaneous estimation of the clock frequency offset and fixed delay. Fig. 4(b) presents the SIB9-sync signaling test results, demonstrating that the designed signaling structure can successfully encap-

```
Universitor = 2076000000 00000 u denominator=2081052000 00000 offset; 0.99714 delay. 2103.95825 delay. 2103.27700.00000 d_denominator=415200000 000000 delay. 2103.95825 delay. 2103.27700.00000 d_denominator=415200000 000000 delay. 2103.95825 delay. 2103.95825 delay. 2103.25825 dela
```

Fig. 4. Function adaptation test result. (a) Timestamp free synchronization test; (b) SIB9-sync signaling test.

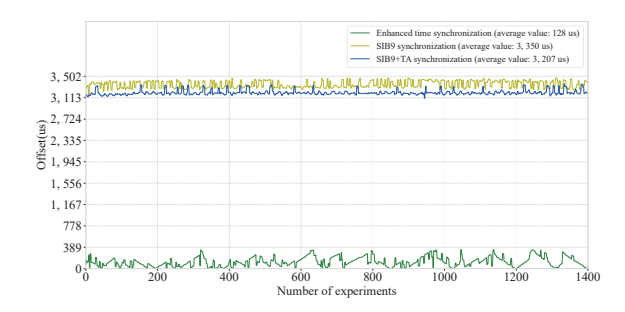


Fig. 5. Time synchronization accuracy test comparison diagram.

sulate synchronization parameters and be correctly interpreted by the UE, thereby validating the effectiveness of the proposed scheme. Upon correctly receiving the SIB9-sync message, the UE records the local reception time to perform one-way clock synchronization and compute the clock phase offset. These experimental results collectively confirm that the proposed time synchronization scheme can be effectively deployed in the NR system, validating both its feasibility and functional stability.

The performance of the improved time synchronization method is evaluated in terms of synchronization accuracy and memory consumption. The proposed improved synchronization algorithm is compared with two existing synchronization methods, as illustrated in Fig. 5. It can be observed that the improved time synchronization method demonstrates a significant advantage in synchronization accuracy, achieving an average accuracy of approximately 128 μ s, and typically maintaining accuracy within 343 μ s.

Subsequently, A comparative analysis of the memory overhead introduced by the improved synchronization method is presented. As shown in Fig. 6(a), the additional RAM usage attributed to the synchronization module increases by approximately 13 MB on the gNB side and by about 23.7 MB on the UE side. Fig. 6(b) illustrates ROM usage, where a marginal increase of 4 KB is observed on the gNB side, while the UE side shows a slight increase of 12 KB. These results demonstrate that the improved method imposes only minimal memory overhead, making it suitable for deployment in resource-constrained industrial devices.

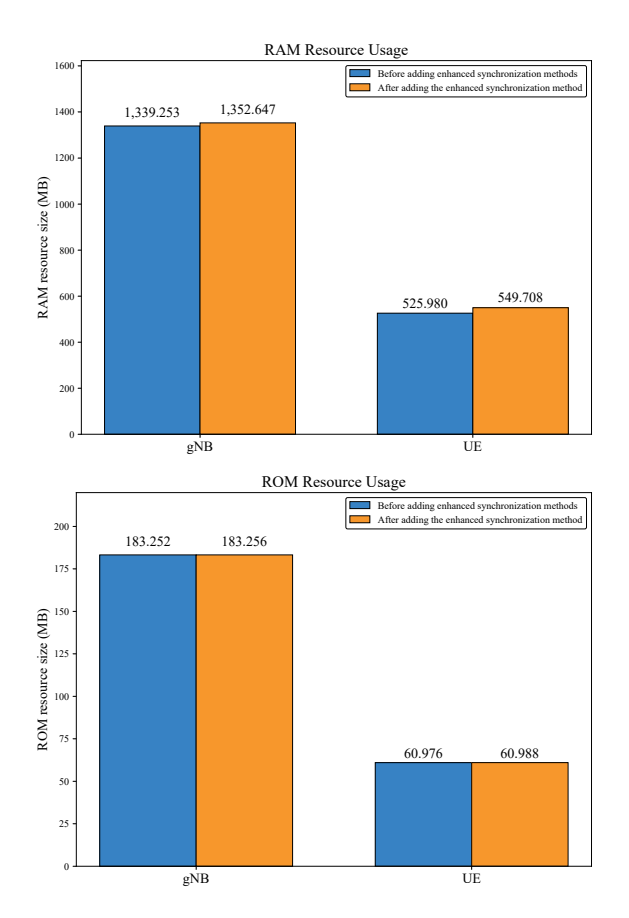


Fig. 6. Resource usage for improved time synchronization. (a) Comparative analysis of RAM resource utilization; (b) Comparative analysis of ROM resource utilization.

V. CONCLUSION

This paper proposes an improved time synchronization method for 5G-A networks, which primarily comprises timestamp-free mechanism, SIB9-sync signaling, and unidirectional clock synchronization. The proposed scheme is implemented on the OAI platform. Experimental results demonstrate that the proposed method significantly improves synchronization accuracy over conventional approaches, meets the performance requirements for high-precision synchronization, and facilitates the development of industrial systems. In the current implementation, the Physical Downlink Shared Channel is used for downlink data transmission, whereas the Physical Uplink Control Channel is used for uplink feedback. This channel configuration results in a path delay asymmetry. To address this asymmetry, future experiments may explore migrating ACK/NACK feedback to the Physical Uplink Shared Channel. By enabling dynamic scheduling, uplinkdownlink path symmetry can be achieved, thereby further improving synchronization accuracy.

REFERENCES

[1] W. Chen, X. Lin, J. Lee, A. Toskala, S. Sun, C. F. Chiasserini, and L. Liu, "5G-Advanced toward 6G: Past, present, and future," *IEEE J. Sel. Areas Commun.*, vol. 41, no. 6, pp. 1592–1619, Jun. 2023.

- [2] T. Wührl, M. T. Baross, S. Gyányi, and P. J. Varga, "5G synchronization problems with GNSS interference," in 6th Int. Conf. Workshop Óbuda on Electr. Power Eng. Budapest, Hungary, Oct. 2023, pp. 149–154.
- [3] Óscar Seijo, I. Val, J. A. López-Fernández, J. Montalban, and E. Iradier, "On the use of white rabbit for precise time transfer in 5G URLLC networks for factory automation applications," in *Proc. IEEE Int. Conf. Ind. Cyber Phys. Syst*, Taipei, Taiwan, May. 2019, pp. 385–390.
- [4] H. Cao, J. Shen, R. Yan, Y. Zhao, W. Xu, and L. Geng, "More robust high precision time synchronization system," in *Proc. IEEE Int. Symp. Precis. Clock Synchronization Meas., Control, Commun*, Tokyo, Japan, Oct. 2024, pp. 1–6.
- [5] M. Gundall, C. Huber, and H. D. Schotten, "Extended reference broadcast infrastructure synchronization protocol in 5G and beyond," in *Proc.* 2023 IEEE 21st Int. Conf. Ind. Informatics, Lemgo, Germany, Jul. 2023, pp. 1–6
- [6] Z. Wang, C. Zhang, W. Zheng, X. Wen, and Z. Lu, "TAPv2: An approach towards sub-microsecond level timing accuracy over air interface," *IEEE Trans. Veh. Technol*, vol. 71, no. 4, pp. 3995–4009, Apr. 2022.
- [7] M. U. Hadi, T. Jacobsen, R. Abreu, and T. Kolding, "5G time synchronization: Performance analysis and enhancements for multipath scenarios," in *Proc. 2021 IEEE Latin-Amer. Conf. Commun*, Santo Domingo, Dominican Republic, Nov. 2021, pp. 1–5.
- [8] A. Mahmood, M. I. Ashraf, M. Gidlund, J. Torsner, and J. Sachs, "Time synchronization in 5G wireless edge: Requirements and solutions for critical-MTC," *IEEE Commun. Mag.*, vol. 57, no. 12, pp. 45–51, Dec. 2019
- [9] Z. Chai, W. Liu, K. Lai, and J. Lei, "Clock synchronization based on physical-layer pulse and timestamp free mechanism in 5G," in *Proc.* 2021 13th Int. Conf. Wireless Commun. Signal Process, Changsha, China, Oct. 2021, pp. 1–5.
- [10] D. Chandramouli, P. Andres-Maldonado, and T. Kolding, "Evolution of timing services from 5G-A toward 6G," *IEEE Access*, vol. 11, pp. 35150– 35157, Apr. 2023.
- [11] Z. Chai, W. Liu, J. Zhu, and J. Lei, "Absolute time synchronization based on timing message exchange in 5G wireless edge," in *Proc. 2021 IEEE 21st Int. Conf. Commun. Technol*, Tianjin, China, Oct. 2021, pp. 538–543.